Optical micro-shadowgraph-based method for measuring micro-solderball height

Shihua Wang
Chenggen Quan
Cho Jui Tay
National University of Singapore
Department of Mechanical Engineering
10 Kent Ridge Crescent
Singapore, 119260

Abstract. An optical micro-shadowgraph for the height measurement of a micro-solderball on a semiconductor wafer is proposed. The micro-shadow image resulting from an oblique illumination onto the protruded solderball/bump on the wafer is clearly captured. Experimental investigation shows that accurate solderball height measurement can be readily obtained. *© 2005 Society of Photo-Optical Instrumentation Engineers.* [DOI: 10.1117/1.1906003]

Subject terms: geometrical optics; metrology; microscopy; optical shadowgraphs; semiconductor wafers; micro-solderballs.

Paper L040542R received Aug. 11, 2004; revised manuscript received Dec. 29, 2004; accepted for publication Feb. 22, 2005; appeared online Feb. 23, 2005; published online May 23, 2005.

The reliability of the solder joint/solderball in the micro-ball grid array (micro-BGA)[1] has been observed to be highly dependent on the height uniformity/coplanarity[2] of the micro-solderballs across the wafer. To obtain the height information from a micro-BGA on a silicon wafer, we explore a simple but effective method using the inherent shadow phenomenon of an object illuminated by an oblique illumination.

Figure 1 shows a schematic of a micro-solderball/bump illuminated by an incident beam of angle θ. The image plane of the CCD sensor in the X-Y plane is parallel to the line AD and perpendicular to the reflected light. A lens would direct the resulting shadow onto the CCD sensor and hence a typical shadow and projection image of a micro-solderball in the X-Y plane can be illustrated as an overlapped shadow pattern. The length of both d and L can be measured, where d is the diameter of the bump and L is the total length across the bump and its shadow. Hence, from Rt ΔACD, we have

$$\sin 2\theta = \frac{\overline{AD}}{\overline{AC}} = \frac{\overline{A'D'}/\beta}{\overline{AC}} = \frac{L/\beta}{\overline{AC}}, \tag{1}$$

$$\overline{AC} = \frac{L}{\beta \cdot \sin 2\theta}, \tag{2}$$

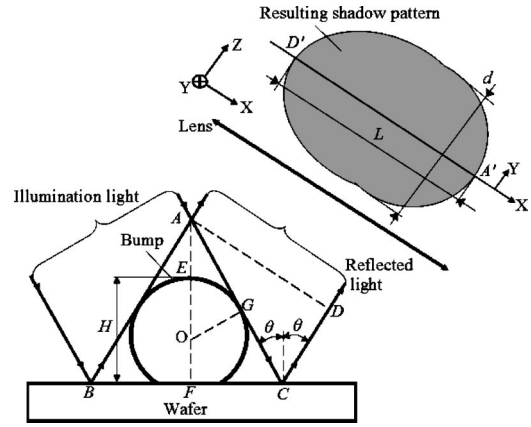

Fig. 1 Cross-section view of the bump and corresponding shadow pattern on the CCD sensor located in the X-Y plane.

where β is magnification of the microscopic system. From Rt ΔAOG,

$$(\overline{AE} + \overline{EO}) \sin\theta = \overline{GO}, \tag{3}$$

where $\overline{EO} = \overline{GO} = d/2\beta$. We have

$$\overline{AE} = \frac{d}{2\beta \cdot \sin\theta} - \frac{d}{2\beta}, \tag{4}$$

and from Rt ΔAFC, we have

$$\overline{AF} = \overline{AC} \cos\theta. \tag{5}$$

Substituting Eqs. (2), (4), and (5) into $H = \overline{AF} - \overline{AE}$, the height of the solderball is given by:

$$H = \frac{1}{2\beta \sin\theta}[L - (1 - \sin\theta) \cdot d]. \tag{6}$$

In Fig. 2, light from a halogen lamp passes through a collimating lens 1 and is directed onto a focusing lens 2. The light beam emerging from lens 2 is focused onto an aperture stop 1. A telecentric illumination consisting of lens 1, lens 2, stop 1, and lens 3 enables illumination with collimated light over the test surface.[3] Note that lens 3 (semi-lens) allows the illumination angle to be easily adjusted by selecting illumination axis offset (P) and most of the light

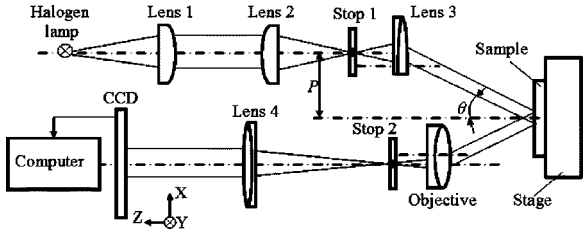

Fig. 2 System configuration.

0091-3286/2005/$22.00 © 2005 SPIE

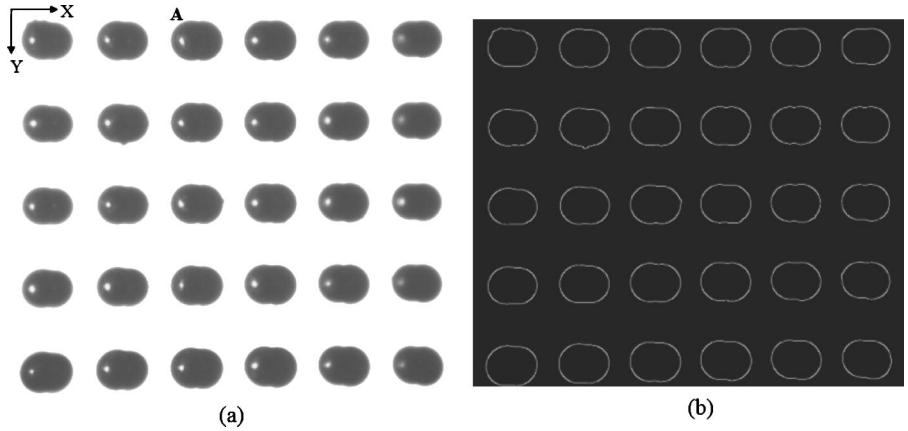

Fig. 3 Results of (a) a shadow image of bumps on a wafer, (b) edge contour of those bumps obtained through image processing using Canny's method.

is reflected in the specular direction as the test surface (silicon wafer) is mirror-like.[4] To capture the resulting shadow pattern, another telecentric microscope consisting of an objective (focal length $f_o = 20$ mm), aperture stop 2, and lens 4 (focal length $f_4 = 100$ mm) is aligned in the specular direction of the reflected light.This arrangement ensures an optimal contrast of the recorded white-black pattern on a CCD sensor Stop 2 located at the focal plane of the lens 4 ensures that rays primarily parallel to the optical axis reach the CCD sensor. The resulting shadow pattern is recorded through a frame grabber for the further processing.

Figure 3(a) shows a typical shadow pattern of micro-solderballs on a wafer. It is seen that those shadows are elongated in the X direction. To determine the shadow contour, Canny's edge method[5] was applied to the above shadow pattern. Figure 3(b) shows the edges/contours of those shadows. As shown in Fig. 3(b), the shadow edges have been located and the corresponding shadow length is correlated to the micro-solderball/bump height. For example, the edge locations across the centroids of a specific bump A and its shadow length along the Y direction have been used to measure the bump diameter $d(=58\,\text{pixels})$ and the elongated shadow along the X direction in a length of $L(=75\,\text{pixels})$ was also obtained. Based on Eq. (6), the bump height of 108 μm was determined. Similarly, individual height of each bump on the wafer can be measured accordingly. For those bumps in Fig. 3, the bump height variation (uniformity/coplanarity) was evaluated using a statistical parameter of standard deviation σ to be ± 4.8 μm. To verify the accuracy of the proposed method, the height (108.2 μm) of bump A was obtained using a commercial WYKO profiler (Model: Wyko NT 3300, a white-light interferometric profiler). Compared to the height (108 μm) obtained by the proposed method, the discrepancy is less than 0.2%. According to the ISO guide,[6] the combined standard uncertainty $u_c(H)$ attributed to H based on Eq. (6) is given as follows:

$$u_c(H) = \left[\left(\frac{\partial H}{\partial L}\right)^2 u_{(L)}^2 + \left(\frac{\partial H}{\partial d}\right)^2 u_{(d)}^2 + \left(\frac{\partial H}{\partial \beta}\right)^2 u_{(\beta)}^2 + \left(\frac{\partial H}{\partial \theta}\right)^2 u_{(\theta)}^2 \right]^{1/2}, \tag{7}$$

where the partial derivatives ($\partial H/\partial L = 0.3$, $\partial H/\partial d = 0.2$, $\partial H/\partial \beta = 22$, and $\partial H/\partial \theta = 137$) for bump A are called sensitivity coefficients, $u_{(L)}$, $u_{(d)}$, $u_{(\beta)}$ and $u_{(\theta)}$ are the standard uncertainties of L, d, β, and θ, respectively. The error resulting from determination of those lengths of L and d are less than 1 pixel (10 μm) which is 2 μm on the test surface while the magnification (β) is 5×. The corresponding standard uncertainties assuming a rectangular distribution are given approximately by $u_{(L)} = u_{(d)} = 2/\sqrt{3} = 1.2\,\mu$m. The magnification ($\beta = 5\times$) is in a tolerance of $\pm 0.05\times$ with standard uncertainty $u_{(\beta)} = 0.05/\sqrt{3} = 0.03\times$. The error resulting from illumination angle uncertainty was estimated to be in the range of ± 1 deg (0.02 rad) and the corresponding standard uncertainty is given by $u_{(\theta)} = 0.02/\sqrt{3} = 0.01$ rad. The combined standard uncertainty $u_c(H)$ in Eq. (7) can be calculated as follows:

$$u_c(H) = (0.3^2 \times 1.2^2 + 0.2^2 \times 1.2^2 + 22^2 \times 0.05^2 + 137^2 \times 0.01^2)^{1/2} = 1.8\ \mu\text{m}. \tag{8}$$

In summary, the proposed microscopic system is feasible to do measurement on the height of the smooth and curved micro-solderball. The results presented in this letter demonstrate the potential of the proposed method to be a practical tool for in-situ inspection of height and coplanarity on a micro-BGA.

References

1. H. M. Clearfield, J. L. Young, S. D. Wijeyesekera, and E. A. Logan, "Wafer-lever chip scale packaging: benefits for integrated passive devices," *IEEE Trans. Adv. Packag.* **23**, 247–251 (2000).
2. D. Miller, "Inspection criteria for ball grid arrays," *EE-Eval. Eng.* **38**, 137–145 (1999).
3. S. H. Wang, C. J. Jin, C. J. Tay, C. Quan, and H. M. Shang, "Design of an optical probe for testing surface roughness and micro-displacement," *Precis. Eng.* **25**, 258–265 (2001).
4. S. H. Wang, C. G. Quan, C. J. Tay, and H. M. Shang, "Surface roughness measurement in the submicrometer range using laser scattering," *Opt. Eng.* **39**, 1597–1601 (2000).
5. D. C. He and L. Wang, "Edge-detection in numerical image-processing," *Int. J. Remote Sens.* **12**, 651–657 (1991).
6. International Organization for Standardization, *Guide to the Expression of Uncertainty in Measurement*, ISO, Geneva (1995).